

PAPER • OPEN ACCESS

The role of heavy metal ions on spin transport in organic semiconductors

To cite this article: B B Chen *et al* 2015 *New J. Phys.* **17** 013004

View the [article online](#) for updates and enhancements.

Related content

- [Strong asymmetrical bias dependence of magnetoresistance in organic spin valves: the role of ferromagnetic/organic interfaces](#)
S W Jiang, D J Shu, L Lin *et al.*
- [Topical Review](#)
W J M Naber, S Faez and W G van der Wiel
- [Muon spin spectroscopy: magnetism, soft matter and the bridge between the two](#)
L Nuccio, L Schulz and A J Drew

Recent citations

- [Charge Transfer from Alq3-5Cl to Graphene Oxide in Donor-Acceptor Heterostructures](#)
Silviu Polosan *et al*
- [Quantum spin Hall effect in two-dimensional hydrogenated SnPb alloy films](#)
Miaojuan Ren *et al*
- [Organic Spin Valves: A Review](#)
Jagannath Devkota *et al*



PAPER

The role of heavy metal ions on spin transport in organic semiconductors

OPEN ACCESS

RECEIVED

27 October 2014

ACCEPTED FOR PUBLICATION

21 November 2014

PUBLISHED

9 January 2015

Content from this work
may be used under the
terms of the [Creative
Commons Attribution 3.0
licence](#).

Any further distribution of
this work must maintain
attribution to the author
(s) and the title of the
work, journal citation and
DOI.

B B Chen¹, S Wang¹, S W Jiang¹, Z G Yu², X G Wan¹, H F Ding¹ and D Wu¹¹ Department of Physics, National Laboratory of Solid State Microstructures, Nanjing University, Nanjing 210093, People's Republic of China² ISP/Applied Sciences Laboratory, Washington State University, Spokane, Washington 99210, USAE-mail: dwu@nju.edu.cn**Keywords:** organic spintronics, spin relaxation, spin orbit coupling, magnetoresistance**Abstract**

It is generally believed that spin-orbit coupling (SOC) strength and the associated spin relaxation can be enhanced by introducing heavy metal ions in organic semiconductors. Here, we systematically study the spin transport in two organic semiconductors, tris(2-phenylpyridine)iridium ($\text{Ir}(\text{ppy})_3$) and tris-(8-hydroxyquinoline) aluminum (Alq_3), which have similar chemical structures except that $\text{Ir}(\text{ppy})_3$ contains a heavy metal ion Ir. As expected, the photoluminescence spectroscopy measurements show that the SOC strength in $\text{Ir}(\text{ppy})_3$ is several orders of magnitude larger than in Alq_3 . Surprisingly, the spin diffusion length in $\text{Ir}(\text{ppy})_3$, deduced from magnetoresistance measurements in $\text{Ir}(\text{ppy})_3$ -based organic spin valves, is longer than in Alq_3 . Considering the lower carrier mobility in $\text{Ir}(\text{ppy})_3$, the spin relaxation time in $\text{Ir}(\text{ppy})_3$ is much longer than in Alq_3 , implying that the SOC strength in $\text{Ir}(\text{ppy})_3$ is weaker than in Alq_3 . The seemingly contradictory results of photoluminescence spectroscopy and magneto-transport can be explained by the SOC strength depending on the electronic states of a material. The weak SOC strength in $\text{Ir}(\text{ppy})_3$ observed in magneto-transport measurements is due to the strong ligand field induced orbital moment quenching for Ir^{3+} and the polarons transporting in the ligands. However, the excitons involved in photoluminescence spectroscopy overlap with the Ir ion and transforms Ir^{3+} to Ir^{4+} , which has non-zero spin and orbital moments and hence results in high SOC strength.

1. Introduction

Spintronics, which utilizes spin degrees of freedom as the ultimate carrier of information, has attracted deep interest over the past few decades [1]. Motivated by the prospect of the practical integration of the mainstream semiconductor industry, semiconductor spintronics has made impressive progress in the past dozen years [2], during which time the field of organic semiconductor (OSC) spintronics has blossomed [3, 4]. However, due to the weak van der Waals interactions between molecules, electron wave functions are mainly localized within a single molecule and barely overlap. The mechanism of charge-carrier transport is, therefore, dominated by hopping and OSCs present very low mobility in comparison with inorganic semiconductors, in which the band transport mechanism dominates. Spin transport is closely related to charge-carrier transport; as a consequence, the spin transport mechanism in OSCs is radically distinct from inorganic systems and rather complicated. The spin-orbit coupling (SOC) and hyperfine interaction (HFI) are generally believed to be the two major sources of spin relaxation. Owing to the constituents of light elements, and C^{12} possessing zero nuclear spin moment, organic materials are characterized by weak SOC and HFI. This makes the spin relaxation time extremely long and OSCs suitable as the spin transport materials. However, the spin diffusion length is very short due to the very low carrier mobility [5]. For instance, the spin diffusion length is about 45 nm in tris-(8-hydroxyquinoline) aluminum (Alq_3) [6] and 13.3 nm in rubrene [7] in comparison to 200 nm in Si [8]. Therefore, the spin relaxation in OSCs still plays an important role in spin-related phenomena.

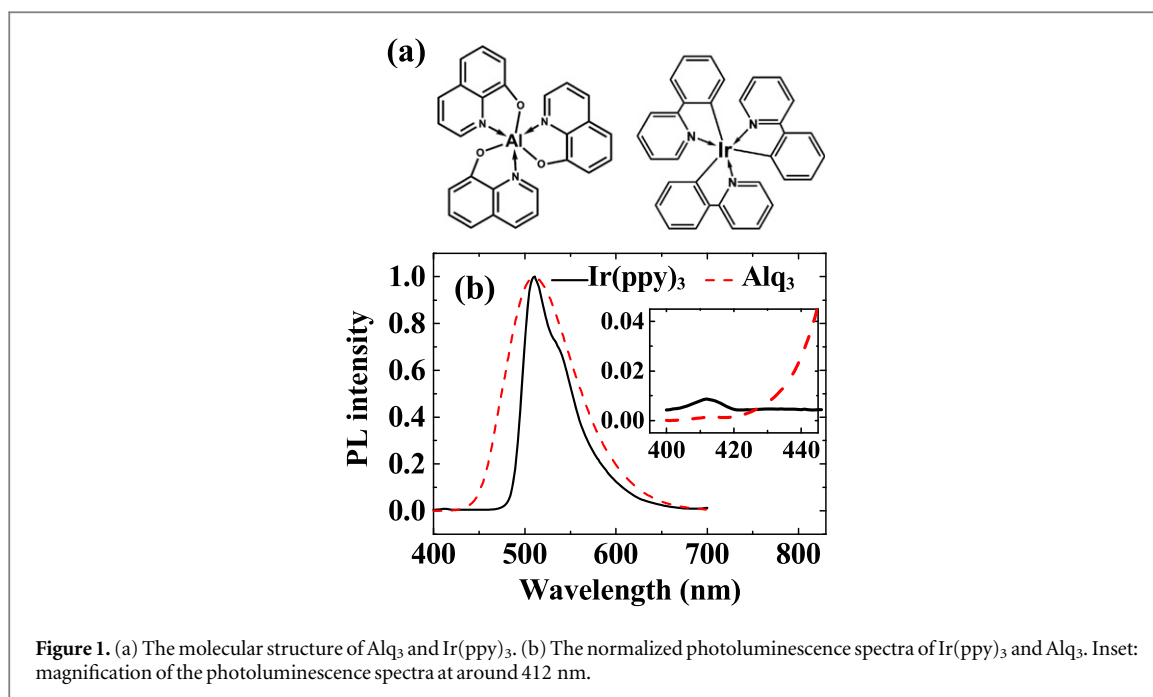
Since the SOC and HFI are both weak, it is difficult to identify which one dominates the spin relaxation and it remains a central issue in organic spintronics [3, 5, 9]. As for HFI, it mainly originates from hydrogen atoms and other atoms possessing a nuclear spin. The carriers experience a random local effective magnetic field, which is the sum of a random effective HFI field and a uniform external magnetic field while hopping between molecules. The spin processes around the random local field on various molecules, giving rise to spin relaxation [10]. Experimental results showing substantially reduced width of magneto-electroluminescence and magnetic resonance, and a significant increase of spin diffusion length after replacing the hydrogen atoms with deuterium atoms in polymers [11] offer direct support for the HFI-induced spin relaxation mechanism. The HFI also plays a crucial role in organic magnetoresistance (OMAR) effects, in which the spin-polarized carrier injection and transport are absent [12].

The SOC mixes opposite spin states and hence the spin-up and spin-down are not good quantum numbers. Therefore, the hopping process accompanies a spin flip event, resulting in spin relaxation. Unlike HFI there are, to date, few experiments that directly support the contribution of SOC to spin relaxation. In the transport study on a Ni/Alq₃/Co nanowire in a strong magnetic field, Pramanik *et al* have recently shown that SOC dominates the spin relaxation rather than HFI in Alq₃ [13]. Yu developed a theory based on SOC-driven spin relaxation and successfully explained the temperature dependence of the spin diffusion length of Alq₃ [14, 15]. Since the SOC strength scales with Z^4 with the atomic number, Z , in atoms, the immediate strategy required to tune the SOC strength in molecules is to introduce heavy ions into molecules. The heavy ion enhanced SOC strength is directly measured by muon spin spectroscopy and time-resolved photoluminescence techniques [16] and appears to play an important role in OMAR effects [17]. In fact, this approach is frequently used in organic light emitting diodes (OLEDs) to enhance the electroluminescence intensity [18]. In luminescence phenomena, the involved electronic states are the excitons. However, in organic spin valves (OSVs), the electronic states responding to transport are spin-polarized polarons rather than excitons. Although the heavy ions can influence the luminescence and excitons, the impact of heavy ions on spin-polarized polarons still needs to be examined.

In this work, we fabricated OSVs using small molecules of tris(2-phenylpyridine)iridium [Ir(ppy)₃] and Alq₃, which have similar chemical structures, as the organic spacers. The Ir(ppy)₃ and Alq₃ molecules exhibit very strong and very weak SOC strength, respectively, according to photoluminescence spectroscopy measurements. If the SOC does affect the spin relaxation, the spin relaxation time in Ir(ppy)₃ would be much shorter than in Alq₃. However, we measured spin diffusion length $\lambda_s \approx 120$ nm for Ir(ppy)₃-based OSVs and $\lambda_s \approx 37$ nm for Alq₃-based OSVs at 10 K. Considering the lower mobility of Ir(ppy)₃, we conclude that the spin relaxation time in Ir(ppy)₃ is longer than in Alq₃, contradictory to photoluminescence spectroscopy measurements. We attribute this unexpected result to the spin-polarized polarons experiencing weak SOC strength in Ir(ppy)₃ because the polarons transport on the ligand, and the ground state of Ir³⁺ ion has a completely quenched orbital moment due to a strong octahedral ligand field, meaning very weak SOC strength. However, photoluminescence spectroscopy is related to the excitons instead of the polarons, which overlap with the Ir ion and transform Ir³⁺ to Ir⁴⁺. The Ir⁴⁺ ion has non-zero spin and orbital moments, suggesting very large SOC strength experienced by the excitons. Our work reveals that the polarons and excitons experience different SOC strength in a material with heavy ions.

2. Experiment

The OSV structure consists of two ferromagnetic electrodes separated by an organic spacer. We used La_{0.67}Sr_{0.33}MnO₃ (LSMO) and Co as bottom and top electrodes, respectively. The LSMO films of about 100 nm were epitaxially grown on SrTiO₃ (001) substrates using pulsed laser deposition (PLD) at 750 °C and 2×10^{-5} Torr oxygen pressure by applying a KrF excimer laser. The laser energy on the polycrystalline LSMO target was 2 J cm^{-2} with a repeat rate of 8 Hz. The growth rate of LSMO films was about 0.08 nm s^{-1} , which was calibrated by monitoring the intensity oscillations of the *in situ* reflection high-energy electron diffraction (RHEED) spot with a laser repetition of 2 Hz [19]. The width of the LSMO electrodes was defined by a shadow mask during PLD. Then the LSMO films were annealed in flowing pure oxygen at atmospheric pressure at 1100 °C for 6 hours to obtain an atomically smooth surface and enhance the magnetic property [20]. The purified Alq₃, Ir(ppy)₃ and platinum octaethylporphyrin (PtOEP) films were thermally evaporated at a rate of 0.07 nm s^{-1} on LSMO electrodes with a base vacuum pressure of 1×10^{-7} Torr. The thickness and growth rate were *in situ* controlled by a quartz crystal thickness monitor next to the samples. A thick organic film was first fabricated to calibrate the thickness monitor by comparison with the Dektek150 surface profiler measurements. Without breaking vacuum, the LSMO/organic bilayers were covered by a shadow mask to define a proper size of the top ferromagnetic layer. The 20 nm-thick top Co electrodes were deposited by a growth method called indirect deposition, which was described in detail in our previous publication [21]. This method



can dramatically reduce the penetration of Co atoms into an organic layer, or the so-called ‘ill-defined’ thickness. The obtained devices were cross-bar geometry with an active area of about $1 \times 1 \text{ mm}^2$. The LSMO films were ultrasonically cleaned using alcohol and acetone, and reused multiple times without apparent degradation in transport measurements. The two sets of Alq₃ and Ir(ppy)₃ based OSVs were fabricated on two different pieces of LSMO film, respectively.

The samples were mounted on a Cooper block cooled by a close-cycle refrigerator located in an electromagnet. The magnetoresistance (MR) responses were measured by a sweeping magnetic field parallel to the film plane. The OSVs with various Alq₃ and Ir(ppy)₃ thickness were carefully studied at a constant voltage to extract the spin diffusion lengths. The photoluminescence spectroscopy of the dissolved Alq₃ and Ir(ppy)₃ in toluene were measured using a Hitachi F-4600 fluorescence spectrophotometer with an excitation wavelength of 367 nm at room temperature.

3. Experimental results

3.1. Photoluminescence spectra

Although the SOC strength is very weak in OSCs, it is generally believed that the presence of a large- Z or heavy ion in OSCs can enhance the SOC strength [22]. To study the role of the SOC in spin transport, we choose two molecules, Alq₃ and Ir(ppy)₃, with similar chemical structure, but one with the light metal ion Al³⁺ ($Z = 13$) and another with the heavy metal ion Ir³⁺ ($Z = 77$), shown in figure 1(a). The SOC strength of Ir(ppy)₃ is expected to be much stronger than that of Alq₃ due to the much heavier Ir³⁺ ion.

The light emission from organic molecules is generated by the transition from the singlet (total spin, $S = 0$) or triplet ($S = 1$) excitons to ground states ($S = 0$), which is known as fluorescence or phosphorescence. Only fluorescence emission is allowed without SOC due to the conservation of the spin angular momentum. However, the presence of the strong SOC can lead to the occurrence of phosphorescence emission because the spin angular momentum is not necessarily conserved. Moreover, due to the triplet state energy being lower than the singlet state energy, the transfer from singlet state to triplet state, known as intersystem crossing (ISC), will occur with strong SOC. Therefore, the relative emission intensity of the fluorescence and phosphorescence, the ISC rate (k_{ISC}) and the SOC strength are intimately correlated.

Figure 1(b) shows the normalized photoluminescence (PL) spectra of Ir(ppy)₃ and Alq₃. Ir(ppy)₃ displays two emission maxima at 511 and 412 nm, which agree well with previous reports and are assigned to the phosphorescence and fluorescence emission, respectively [17, 23]. The much stronger phosphorescence peak indicates that excitons experience a very large SOC strength. From the rate equations, the intensity ratio between phosphorescence and fluorescence can be written as,

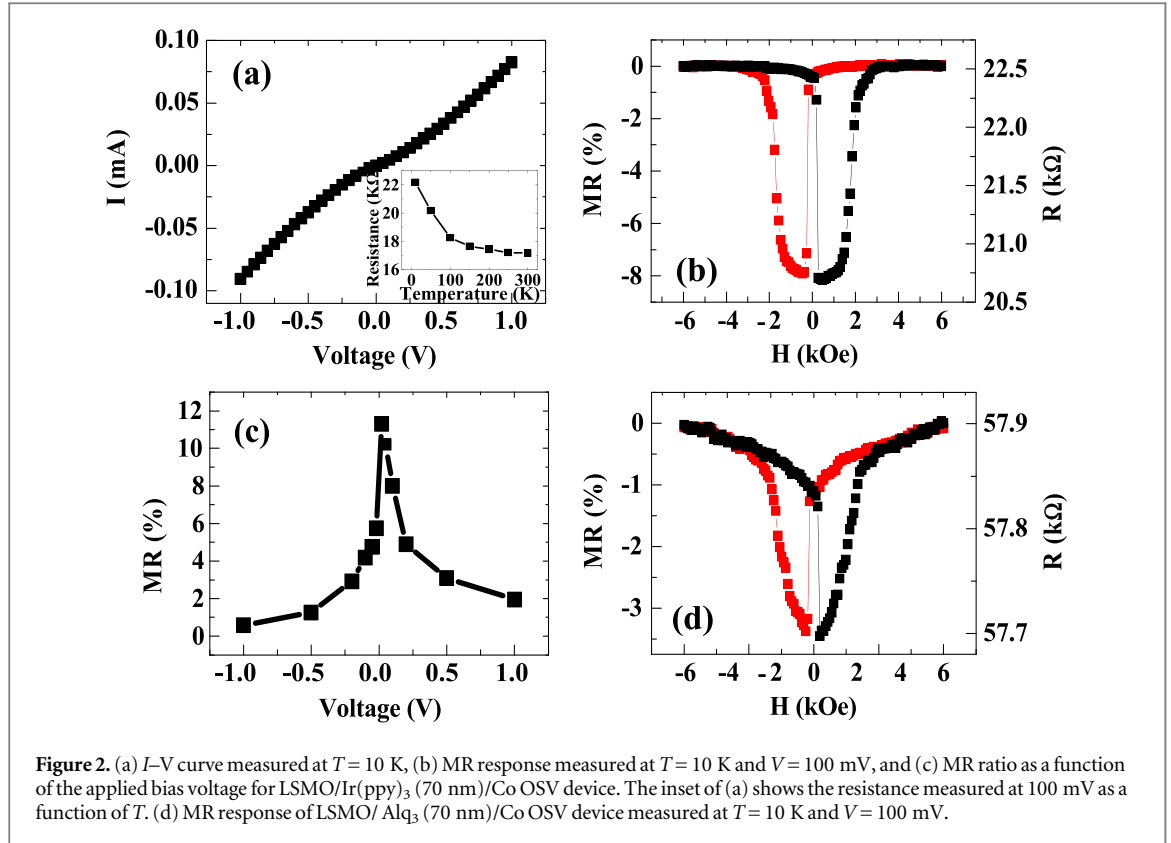


Figure 2. (a) I - V curve measured at $T = 10$ K, (b) MR response measured at $T = 10$ K and $V = 100$ mV, and (c) MR ratio as a function of the applied bias voltage for LSMO/Ir(ppy)₃(70 nm)/Co OSV device. The inset of (a) shows the resistance measured at 100 mV as a function of T . (d) MR response of LSMO/Alq₃(70 nm)/Co OSV device measured at $T = 10$ K and $V = 100$ mV.

$$\frac{I_P}{I_F} = k_{\text{ISC}} \tau_S^* \frac{\eta_P \hbar \omega_P}{\eta_F \hbar \omega_F}, \quad (1)$$

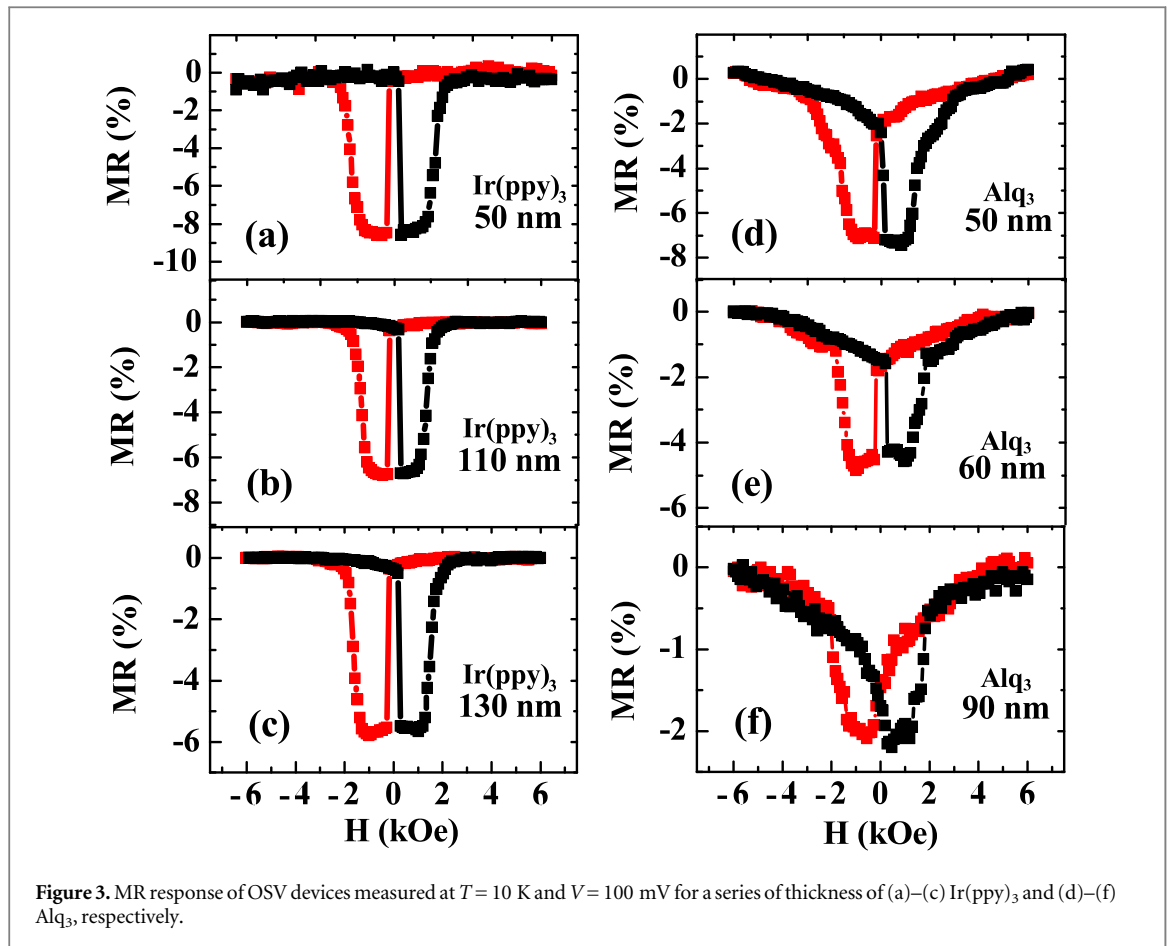
where I_P and I_F are the phosphorescence and fluorescence intensity, respectively; $\hbar \omega_P$ and $\hbar \omega_F$ are the phosphorescence and fluorescence photon energy, respectively; η_P and η_F are the singlet and triplet emission quantum efficiency, respectively; τ_S^* is the singlet lifetime while assuming $k_{\text{ISC}} = 0$. For the order of magnitude estimation, we assume $\eta_P/\eta_F \approx 1$ and $\tau_S^* = 14$ ns, for which the Alq₃ singlet lifetime is adopted [24]. Therefore, the k_{ISC} of Ir(ppy)₃ is extracted to be $1.7 \times 10^4 \mu \text{s}^{-1}$ according to equation (1) and the PL spectrum of Ir(ppy)₃, consistent with previous reports [17].

Alq₃ exhibits only one emission peak at 510 nm with no additional structures, which originates from the fluorescence emission [25]. The phosphorescence emission is not observed, indicating that the SOC strength is very weak. Although we did not get the k_{ISC} value of Alq₃ from PL measurements, k_{ISC} of Alq₃ was measured by the time-resolved photoluminescence technique to be of the order of $1.7 \mu \text{s}^{-1}$ [26]. Since k_{ISC} is proportional to the SOC strength [27], these results clearly suggest that the SOC strength in Ir(ppy)₃ is four orders of magnitude larger than in Alq₃. In fact, the effective SOC field is estimated to be ~ 1000 Oe in Ir(ppy)₃ from the uncertainty relationship, and negligible in Alq₃ by fitting OMAR curves [17].

3.2. Transport measurements

According to the above results that the SOC strength in Ir(ppy)₃ is much greater than in Alq₃, it is interesting to compare the spin transport in these two molecules. Since the results in Alq₃ have been reported in detail elsewhere [6, 20, 21], we mainly show the results of Ir(ppy)₃. Figure 2(a) shows the typical current-voltage (I - V) characteristics of LSMO/Ir(ppy)₃(70 nm)/Co OSV at temperature $T = 10$ K. The positive bias voltage means that the current flows from the Co electrode through OSC to the LSMO electrode. The I - V response exhibits a non-linear behavior, indicating the carriers transporting through Ir(ppy)₃ rather than pinholes. The resistance is typically more than 10 k Ω , similar to the Alq₃-based OSV. The device resistance decreases with increasing temperature (inset of figure 2(a)), indicating a semiconducting behavior. Nonlinear I - V curves and the semiconducting behaviors are observed in all samples when varying the organic thickness. These results are similar to previous reports in Alq₃-based OSVs [6, 28–31], suggesting that the conducting mechanism of the Ir(ppy)₃-based OSVs is the same as Alq₃-based OSVs, i.e., hopping transport.

The typical MR curve of LSMO/Ir(ppy)₃(70 nm)/Co OSV is shown in figure 2(b), which was measured at $T = 10$ K and bias voltage $V = 100$ mV. The MR ratio is defined as $MR = \Delta R/R_P = (R_{\text{AP}} - R_P)/R_P$, where R_P and R_{AP} denote the junction resistance in the parallel and anti-parallel magnetization configuration for the two FM

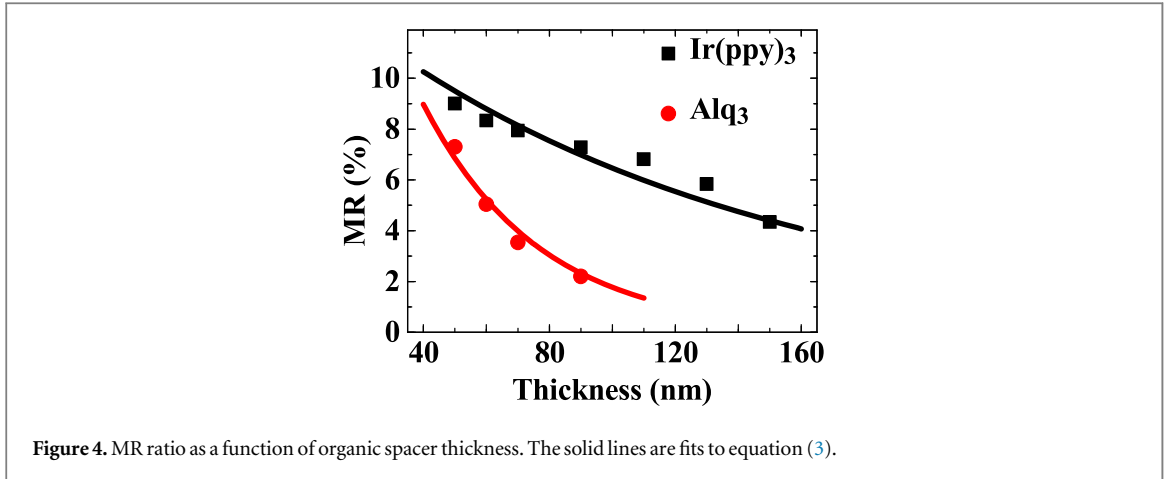


electrodes, respectively. It is clearly seen $R_{AP} < R_P$ in all bias ranges, shown in figure 2(c), i.e., an inverted or negative MR, similar to many other OSVs using LSMO and Co as electrodes, for the organic layer thickness above the tunneling region [3, 6, 20, 32]. In figure 2(c), it is seen that the MR ratio peaks around zero bias voltage and it decreases faster at negative V . These characteristics are similar to Alq₃-based OSVs [6, 21]. For comparison, here we fabricated the OSV of LSMO/Alq₃ (70 nm)/Co and measured the MR curve at $T = 10$ K and $V = 100$ mV, as shown in figure 2(d), in which the LSMO electrode is the same piece of film as the OSV device shown in figures 2(a)–(c). The MR ratio of Ir(ppy)₃-based OSV is about two times larger than that of Alq₃-based OSV.

The demonstration of the Hanle effect is a convincing proof of spin injection into non-magnetic materials [33]. Several unsuccessful attempts have been made to demonstrate the Hanle effect in OSVs, including in Alq₃-based OSVs [34, 35]. Here, we also did not find the Hanle effect in LSMO/Ir(ppy)₃/Co OSVs. This might be due to much faster spin transport than carrier mobility due to the exchange between localized carriers. A magnetic field larger than the electrode saturation field is needed to observe the Hanle effect, leading to the unobservable Hanle effect [36].

3.3. Spin diffusion lengths of Alq₃ and Ir(ppy)₃

MR ratio is determined by the spin polarization, spin diffusion length and spin injection efficiency, etc. However, spin relaxation is only related to spin diffusion length. In order to understand the spin relaxation mechanism, we tried to extract spin diffusion length λ_s by measuring the MR ratio of OSVs with various OSC thicknesses. In these experiments, the same piece of LSMO film was used to fabricate OSVs for each set of samples, considering that the surface property of LSMO is critical to MR ratio and may vary from sample to sample [20]. Figure 3 displays the MR loops of a series of OSVs based on various thicknesses of Alq₃ and Ir(ppy)₃, measured at $T = 10$ K and $V = 100$ mV. Obviously, the MR ratio of the Ir(ppy)₃-based OSVs is larger than that of the Alq₃-based OSVs for the same organic spacer thickness and the MR ratio of the Ir(ppy)₃-based OSVs decreases much slower than that of the Alq₃-based OSVs as OSC layer thickness increases. In OSVs, the MR ratio can be expressed by the modified Jullière formula [6, 11]



$$\text{MR ratio} = \frac{2R_1P_2e^{-d/\lambda_s}}{1 + R_1P_2e^{-d/\lambda_s}}, \quad (2)$$

where d is the thickness of Alq₃ or Ir(ppy)₃, and P_1 and P_2 are the spin polarizations at LSMO/OSC and Co/OSC interfaces, respectively. In our experimental results, MR ratio \ll 100%, equation (2) can be simplified to

$$\text{MR ratio} \approx 2R_1P_2e^{-d/\lambda_s}, \quad (3)$$

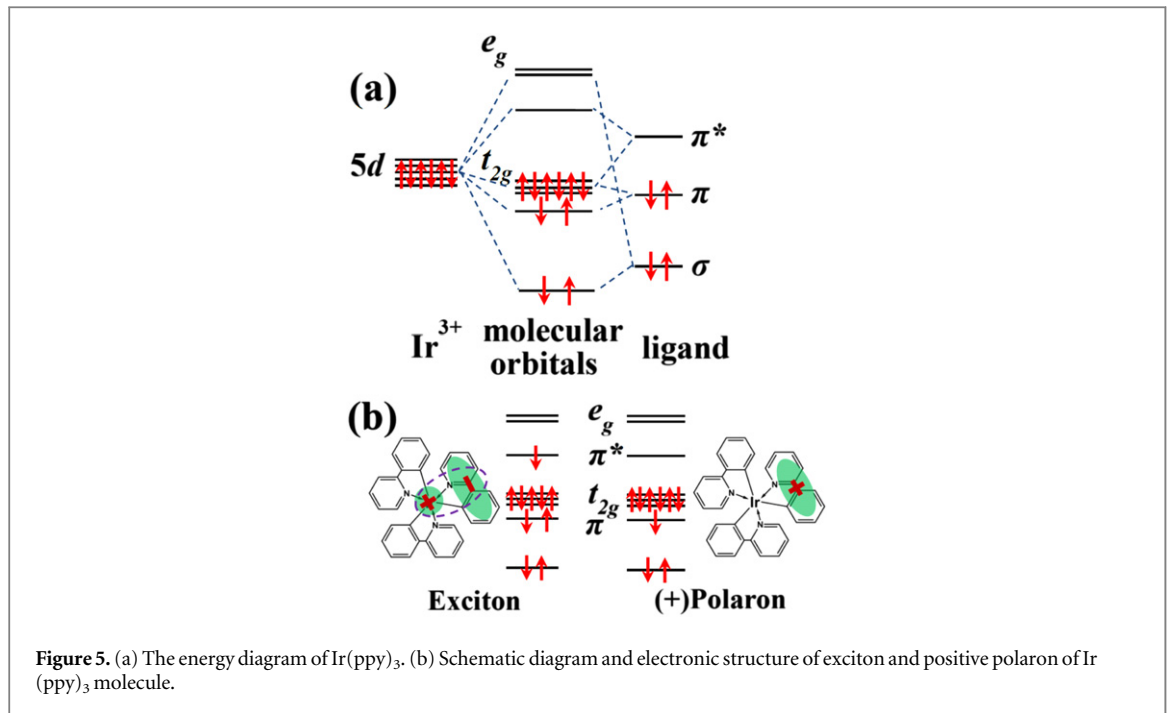
indicating that the MR ratio decreases exponentially as the thickness of the organic spacer increases. We can therefore obtain $\lambda_s = 120$ nm in Ir(ppy)₃ and $\lambda_s = 37$ nm in Alq₃ by fitting MR ratio as a function of Ir(ppy)₃ and Alq₃ thickness in figure 4 to equation (3). The obtained λ_s in Alq₃ is in agreement with previous reports [6]. Thus, as λ_s in Ir(ppy)₃ is found to be larger than λ_s in Alq₃, and considering slower mobility of Ir(ppy)₃ [37, 38], we can immediately conclude that the spin relaxation time in Ir(ppy)₃ is longer than in Alq₃.

4. Discussion

Because the SOC strength in Ir(ppy)₃ is several orders of magnitude larger than in Alq₃ according to the PL measurements, the spin relaxation time in Ir(ppy)₃ should be much shorter than in Alq₃ if the SOC is the main source of the spin relaxation. This expectation is obviously opposite to our results of MR measurements. There are three possible explanations for the unexpected results. (i) Both the HFI and SOC contribute to the spin relaxation. Although the SOC strength in Ir(ppy)₃ is stronger than in Alq₃, the HFI in Ir(ppy)₃ may be much weaker. The overall effects of the HFI and SOC induced spin relaxation in Ir(ppy)₃ can be weaker than in Alq₃. (ii) The spins do not experience strong SOC in Ir(ppy)₃ in the transport experiment, even though strong SOC is observed in the PL measurements. (iii) The SOC does not play a role in the spin relaxation.

The HFI is mainly contributed by the hydrogen nuclei. Since these two molecules have very similar molecular structure and owing to the location of hydrogen atoms, the HFI strength between carriers and hydrogen nuclei should be comparable. Indeed, the effective HFI field of these two molecules was estimated to be about 50 Oe from OMAR measurements [17]. Moreover, a recent theoretical calculation shows that the effective HFI field is 4.1–8.7 Oe in Ir(ppy)₃ and 12.2–12.4 Oe in Alq₃, and which varies due to the different carrier type and the detailed molecular structures [39]. Both the experimental measurements and theoretical calculations reveal that the effective HFI field in Alq₃ and Ir(ppy)₃ is comparable and well below 100 Oe. The effective SOC fields are 1000 Oe in Ir(ppy)₃ and well below 10 Oe in Alq₃ from PL and OMAR measurements, respectively [17]. The overall effective field of the HFI and SOC in Ir(ppy)₃ should be much stronger than in Alq₃. Thus the first possible explanation is not applicable.

Next, we discuss the second possible explanation. Since the PL and magneto-transport measurements involve different electronic states, excitons and polarons, respectively, the heavy ions may have a different impact on these two states. For a molecule with a transition metal ion, the transition metal ion is coordinated with one or more organic ligands. Ir(ppy)₃ is a 5d transition metal octahedral complex with one nitrogen atom and one carbon atom from each ligand bonded to the central metal ion to construct octahedral geometry, shown in figure 1(a), which leads to the d orbitals splitting into a doubly degenerate e_g level with higher energy and a triply degenerate t_{2g} level with lower energy, as shown in the energy diagram of Ir(ppy)₃ in figure 5(a). Due to the large energy splitting of e_g and t_{2g} levels, the t_{2g} level is fully filled with 6d electrons of Ir³⁺ to form a zero spin and zero orbital moment configuration, thus, the SOC strength is negligible for Ir(ppy)₃ in its ground state.



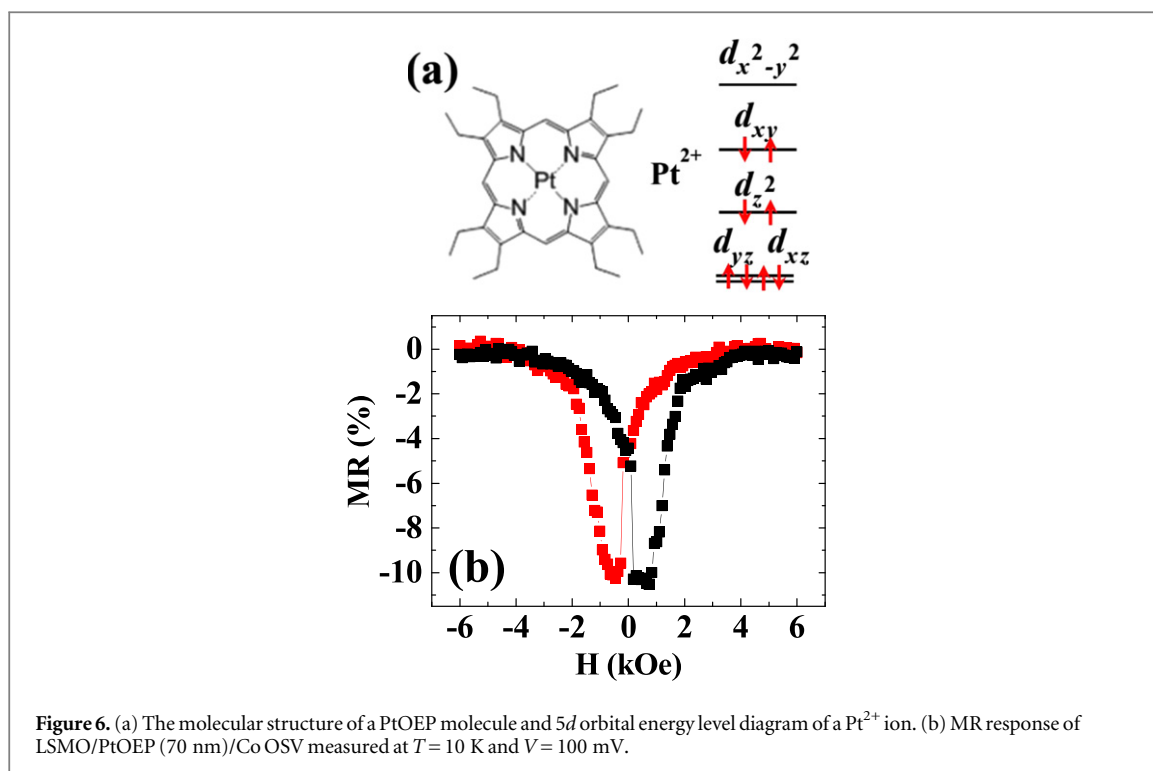
When a polaron is introduced into a Ir(ppy)₃ molecule in a magneto-transport measurement, it mainly localizes and transports on the itinerant π orbitals of the ligands and the inner Ir³⁺ ion remains unchanged, schematically shown in figure 5(b), indicating that the heavy Ir³⁺ ion has an indirect impact on the polarons. Considering the very weak SOC strength of the Ir³⁺ ion, the polarons should not experience strong SOC from the Ir³⁺ ion.

However, in the phenomena with light emission process, such as PL and electroluminescence, a high SOC strength is always observed in Ir(ppy)₃ [40]. In the light emission process, the emission is a transition of an exciton, which is assigned to the metal-to-ligand-charge-transfer (MLCT) state in Ir(ppy)₃, a bound state of an electron localized on the ligand and a hole from the 5d orbital of the Ir⁴⁺ ion, schematically shown in figure 5(b) [41]. Therefore, the Ir ion participates in the light emission and the exciton transforms Ir³⁺ into Ir⁴⁺ in the MLCT state. Because Ir⁴⁺ is a d⁵ configuration, 5 electrons are filled in the t_{2g} level with one uncompensated spin, i.e., non-zero spin and orbital moment. Accordingly, the SOC strength is increased due to the heavy Ir atom and plays a significant role in the light emission process. Therefore, the Ir ion enhanced SOC strength can be observed in the phenomena with light emission.

According to the above analysis, the SOC strength in transport for both molecules is weak. It is difficult to judge whether the SOC plays a role in the spin relaxation from the comparison of these two molecules. Therefore, the third possibility needs further experiments to clarify. We propose choosing molecules with heavy atoms contributing to π -orbitals such as triethylsilylethynyl anthradithiophene (TES-ADT) and triethylsilylethynyl anthradiselenophene (TES-ADS), in which oxygen is replaced by sulfur and selenium [16].

In molecule complexes, the ligand field is usually very strong, resulting in the quenching of the orbital moment and consequently very weak SOC strength at the ground state. Therefore, the weak SOC strength in a molecule with a heavy transition atom should be generally observed in the magneto-transport measurement. To further demonstrate the above scenario, another typical molecule, PtOEP, which shows strong SOC in light emitting phenomena due to a heavy Pt ion [42], was used as an organic spacer to fabricate LSMO/PtOEP (70 nm)/Co OSVs. PtOEP is a 5d transition metal with planar square complexes. d orbitals are split into four energy levels by the planar square ligand field, as shown in figure 6(a). Owing to the strong ligand field, the d orbitals split into four energy levels. The orbital moment of Pt²⁺ d-electrons is quenched, leading to the weak SOC. Indeed, we observed a MR ratio of 11% in the LSMO/PtOEP (70 nm)/Co OSV device at T = 10 K and V = 100 mV, shown in figure 6(b), comparable to Alq₃-based OSVs. This result is consistent with our expectation of weak SOC in PtOEP.

We note that the resistance switching around low coercive field for the Ir(ppy)₃-based OSVs is much sharper than that for the Alq₃-based OSVs, shown in figure 3. According to HFI-induced spin relaxation, the spin diffusion length depends on magnetic field [10], resulting in the curvature of resistance around zero field. The sharper switching suggests smaller HFI strength, in agreement with the theoretical calculation that the HFI in Ir(ppy)₃ is smaller than in Alq₃ by roughly a factor of two [39]. Considering that the SOC strength is low in both



molecules in spin transport, this feature suggests the HFI is the dominant spin relaxation mechanism in these two molecules.

5. Conclusion

We have systematically studied the MR in OSVs with $\text{Ir}(\text{ppy})_3$ and Alq_3 as spacers, which have similar chemical structures. Owing to the heavy Ir ion, the SOC in $\text{Ir}(\text{ppy})_3$ is expected to be much stronger than in Alq_3 and play a significant role in spin relaxation. Indeed, the SOC strength in $\text{Ir}(\text{ppy})_3$ estimated from the PL spectra is four orders of magnitude larger than in Alq_3 . Surprisingly, we found that the MR ratio of $\text{Ir}(\text{ppy})_3$ -based OSVs is higher than that of Alq_3 -based OSVs for the same thickness of organic spacer. From the MR thickness dependence, the spin diffusion lengths in $\text{Ir}(\text{ppy})_3$ and Alq_3 are estimated to be 120 and 37 nm, respectively, suggesting that the heavy Ir ion does not affect the spin transport, unlike in PL. We explain this result as due to the paired electrons and quenched orbital moment by the ligand fields giving nearly zero SOC strength for ground state $\text{Ir}(\text{ppy})_3$. However, in PL, the light emission originates from the transition of the excitons, in which Ir^{3+} is transferred to Ir^{4+} , implying unpaired spin and unquenched orbital moment and hence strong SOC. Our results reveal that the polarons and excitons experience different SOC strength in a material. This scenario is further demonstrated in PtOEP-based OSVs.

Acknowledgments

This work is supported by the National Basic Research Program of China (2010CB923402 and 2013CB922103), the NSF of China (11222435, 51471086 and 11023002) and the NSF of Jiangsu Province (BK20130054).

References

- [1] Wolf S A, Awschalom D D, Buhrman R A, Daughton J M, Molnar S V, Roukes M L, Chtchelkanova A Y and Treger D M 2001 *Science* **294** 1488
- [2] Zutic I, Fabian J and Sarma S D 2004 *Rev. Mod. Phys.* **76** 323
- [3] Dediu V A, Hueso L E, Bergenti I and Taliani C 2009 *Nat. Mater.* **8** 707
- [4] Jiang S W, Yue F J, Wang S and Wu D 2013 *Sci. China-Phys. Mech. Astron.* **56** 142
- [5] Sanvito S 2011 *Chem. Soc. Rev.* **40** 3336
- [6] Xiong Z H, Wu D, Vardeny Z V and Shi J 2004 *Nature* **427** 821
- [7] Shim J H, Raman K V, Park Y J, Santos T S, Miao G X, Satpati B and Moodera J S 2008 *Phys. Rev. Lett.* **100** 226603
- [8] van't Erve O M J, Friedman A L, Cobas E, Li C H, Robinson J T and Jonker B T 2012 *Nat. Nanotechnol.* **7** 737
- [9] Harmon N J and Flatté M E 2013 *Phys. Rev. Lett.* **110** 176602

- [10] Bobbert P A, Wagemans W, van Oost F W A, Koopmans B and Wohlgenannt M 2009 *Phys. Rev. Lett.* **102** 156604
- [11] Nguyen T D, Hukic-Markosian G, Wang F, Wojcik L, Li X-G, Ehrenfreund E and Vardeny Z V 2010 *Nat. Mater.* **9** 345
- [12] Francis T L, Mermer Ö, Veeraraghavan G and Wohlgenannt M 2004 *New J. Phys.* **6** 185
- [13] Pramanik S, Bandyopadhyay S, Garre K and Cahay M 2006 *Phys. Rev. B* **74** 235329
- [14] Yu Z G 2011 *Phys. Rev. Lett.* **106** 106602
- [15] Yu Z G 2012 *Phys. Rev. B* **85** 115201
- [16] Nuccio L et al 2013 *Phys. Rev. Lett.* **110** 216602
- [17] Sheng Y, Nguyen D T, Veeraraghavan G, Mermer Ö and Wohlgenannt M 2007 *Phys. Rev. B* **75** 035202
- [18] Baldo M A, Thompson M E and Forrest S R 2000 *Nature* **403** 750
- [19] Shi Y J, Zhou Y, Ding H F, Zhang F M, Pi L, Zhang Y H and Wu D 2012 *Appl. Phys. Lett.* **101** 122409
- [20] Chen B B, Zhou Y, Wang S, Shi Y J, Ding H F and Wu D 2013 *Appl. Phys. Lett.* **103** 072402
- [21] Wang S, Shi Y J, Lin L, Chen B B, Yue F J, Du J, Ding H F, Zhang F M and Wu D 2011 *Synth. Met.* **161** 1738
- [22] Wilson J, Dhoot A, Seeley A, Khan M, Köhler A and Friend R 2001 *Nature* **413** 828
- [23] Kawamura Y, Goushi K, Brooks J, Brown J J, Sasabe H and Adachi C 2005 *Appl. Phys. Lett.* **86** 071104
- [24] Sokolik I, Priestley R, Walser A D, Dorsinville R and Tang C W 1996 *Appl. Phys. Lett.* **69** 4168
- [25] Pohl P and Anzenbacher P 2003 *Org. Lett.* **5** 2769
- [26] Zhang S, Song J Y, Kreouzis T and Gillin W P 2009 *J. Appl. Phys.* **106** 043511
- [27] Beljonne D, Shuai Z, Pourtois G and Bredas J L 2001 *J. Phys. Chem. A* **105** 3899
- [28] Zhang X, Mizukami S, Kubota T, Ma Q, Oogane M, Naganuma H, Ando Y and Miyazaki T 2013 *Nat. Commun.* **4** 1392
- [29] Rybicki J, Lin R, Wang F, Wohlgenannt M, He C, Sanders T and Suzuki Y 2012 *Phys. Rev. Lett.* **109** 076603
- [30] Schulz L et al 2011 *Nat. Mater.* **10** 39
- [31] Wang F J, Yang C G, Vardeny Z V and Li X G 2007 *Phys. Rev. B* **75** 245324
- [32] Dediu V et al 2008 *Phys. Rev. B* **78** 115203
- [33] Lou X, Adelman C, Crooker S A, Garlid E S, Zhang J, Reddy K S M, Flexner S D, Palmstrom C J and Crowell P A 2007 *Nat. Phys.* **3** 197
- [34] Grünewald M, Göckeritz R, Homonnay N, Würthner F, Molenkamp L W and Schmidt G 2013 *Phys. Rev. B* **88** 085319
- [35] Riminucci A, Prezioso M, Pernechele C, Graziosi P, Bergenti I, Cecchini R, Calbucci M, Solzi M and Dediu V A 2013 *Appl. Phys. Lett.* **102** 092407
- [36] Yu Z G 2013 *Phys. Rev. Lett.* **111** 016601
- [37] Fong H H and So S K 2006 *J. Appl. Phys.* **100** 094502
- [38] Matsusue N, Suzuki Y and Naito H 2005 *Japan. J. Appl. Phys.* **44** 3691
- [39] Yu Z G 2013 *Phys. Rev. B* **87** 205446
- [40] Wu Y, Xu Z, Hu B and Howe J 2007 *Phys. Rev. B* **75** 035214
- [41] Hedley G J, Ruseckas A and Samuel I D W 2008 *Chem. Phys. Lett.* **450** 292
- [42] Baldo M A, O'Brien D F, You Y, Shoustikov A, Sibley S, Thompson M E and Forrest S R 1998 *Nature* **395** 151